Ionization of Rb Rydberg atoms in the attractive *nsnp* dipole-dipole potential

Hyunwook Park, E. S. Shuman, and T. F. Gallagher
Department of Physics, University of Virginia, Charlottesville, Virginia 22904-0714, USA
(Received 26 July 2011; published 9 November 2011)

We have observed the ionization of a cold gas of Rb Rydberg atoms which occurs when *nsns* van der Waals pairs of *ns* atoms of $n \approx 40$ on a weakly repulsive potential are transferred to an attractive dipole-dipole *nsnp* potential by a microwave transition. Comparing the measurements to a simple model shows that the initial 300-μK thermal velocity of the atoms plays an important role. Excitation to a repulsive dipole-dipole potential does not lead to more ionization on a 15-μs time scale than leaving the atoms in the weakly repulsive *nsns* state. This observation is slightly surprising since a radiative transition must occur to allow ionization in the latter case. Finally, by power broadening of the microwave transition, to allow transitions from the initial *nsns* state to the *nsnp* state over a broad range of internuclear spacings, it is possible to accelerate markedly the evolution to a plasma.

DOI: 10.1103/PhysRevA.84.052708 PACS number(s): 34.20.Cf, 34.20.Gj

I. INTRODUCTION

A cold gas of bound Rydberg atoms can spontaneously evolve into an ultracold plasma [1–3]. The mechanism by which it occurs is that a few atoms are ionized by, for example, blackbody photoionization or collisions, and when enough, typically 1%, of the atoms are ionized the macroscopic charge of the cold ions traps all subsequently produced electrons. The trapped electrons initiate a collisional avalanche which rapidly redistributes the Rydberg atom population up and down in energy from the initially populated state, the result being an ultracold plasma and more deeply bound Rydberg atoms. An aspect of the evolution to a plasma which is not completely understood is the initial production of ions, a process which proceeds more rapidly at high n than at low n. Here n is the principal quantum number of the Rydberg atom. Blackbody photoionization rates decrease with n [4], so that at high n the initial ionization is likely to be due to the interaction between atoms. One such mechanism is an ionizing collision of atoms which, while initially at or near rest, are accelerated by attractive or repulsive dipole-dipole forces and collide to produce an ion and a more deeply bound atom, both of which are likely to be moving quickly [5]. Typically, pairs of laser excited atoms have van der Waals $1/R^6$ potentials at long range, where R is the separation between the two atoms. For example, two Rb atoms each in the atomic $40d$ state are in the $40d40d$ diatomic state. At very large separations, for which the dipole-dipole interaction energy is small compared to the energy difference between the $40d40d$ and the nearby $42p38f$ state the potential is a van der Waals $1/R^6$ potential, but at small separations, comparable to the spacing between atoms in the trap, the dipole-dipole interaction exceeds the spacing between the energy levels, and the potential becomes a $1/R^3$ dipole-dipole potential [6]. At very small separations the higher-order multipole interactions become important, and they can affect the dynamics, as pointed out by Cabral *et al.* [7]. Specifically, these interactions can influence the probability of an ionizing collision, but they do not affect the time required for a collision. The time is determined by the longer-range dipole-dipole interaction. Since our atoms are excited at relatively long range, when they encounter avoided crossings due to higher multipoles at short range, they are moving quickly, with the result that the crossings are likely to be traversed diabatically. For this reason, and to keep our model of the process as simple as possible, we only consider the dipole-dipole interactions.

Previous experiments have shown that laser excitation to attractive diatomic potentials is far more likely to lead to ions than excitation to flat or repulsive potentials [6,8,9]. In particular, Amthor *et al.* showed that when Rb atoms are excited to the attractive *ndnd* potentials, the maximum number of ions produced occurs at frequencies below the $R = \infty$ frequencies, that is, when the excitation is to pairs of atoms which are relatively close together on an attractive potential [8]. They also observed enhanced ionization rates when close pairs of atoms on a repulsive van der Waals potential are excited [10]. In particular, in the latter case they noted that the maximum number of ions is found with the exciting laser tuned to the blue of the $R = \infty$ frequency.

Laser excitation leads to the production of pairs of atoms with a range of separations, which depend on the potentials of the Rydberg atom pairs and the linewidth of the exciting laser. Both the distribution of the spacings and the repulsive or attractive nature of the potentials can contribute to ionization, and these two effects are difficult to disentangle. Here we report an experiment in which we separate these effects. Pairs with the same distributions of spacings are placed on flat, attractive, or repulsive potentials. Specifically, we excite Rb atoms to *ns* states of $n = 40$ and $n = 41$ with a pulsed laser, producing pairs of atoms on the very weakly repulsive, essentially flat, *nsns* van der Waals potentials. Since the *nsns* potential is relatively flat, pairs of atoms with a broad range of internuclear spacings can be excited with a single narrow-band laser, which is not possible with very attractive or repulsive potentials [11]. Of course, if the transition is power broadened, it is possible to excite atoms with small internuclear spacings with a narrow-band laser [12]. The atoms are then transferred to attractive or repulsive *nsnp* potentials with a microwave pulse, and we observe the subsequent evolution as a function of time. Specifically, we drive transitions from the $ns_{1/2}ns_{1/2}$ potentials to the $ns_{1/2}np_{1/2}$ potentials, which for simplicity we label as *nsnp* potentials. We observe that microwave excitation to the attractive potentials leads to enhanced ionization, while

excitation to the repulsive potential has no discernible effect. Our observations of the ionization can be reproduced with a simple model when the initial thermal motion of the atoms is taken into account.

II. EXPERIMENTAL APPROACH

The essential idea of the experiment is shown in Fig. 1. Rb $5p_{3/2}$ atoms in a vapor-loaded magneto-optical trap (MOT) are excited to the ns state at a 20-Hz repetition rate by a 480-nm laser pulse. The laser excitation of ns atoms creates pairs of ns atoms with random internuclear spacings, as shown in Fig. 1(a). Subsequent to the pulsed laser excitation, pairs of atoms can be driven to the $nsnp$ or $ns(n-1)p$ state by a 500-ns long microwave pulse to either an attractive or repulsive potential. The transition to the attractive (repulsive) $nsnp$ potential occurs at microwave frequencies below (above) the atomic ns-np frequency, and the transition to the attractive (repulsive) $ns(n-1)p$ potential occurs at microwave frequencies above (below) the atomic ns-$(n-1)p$ frequency. Atoms excited to the attractive and repulsive potentials begin to move due to the dipole-dipole force, and they are allowed to move for a time τ, as shown by Fig. 1(b). After a time delay τ a field ionization pulse with a risetime of 3 μs is applied, and the resulting ions are driven to the microchannel plate (MCP) detector. In Fig. 1(b) we show the time-resolved MCP signal which results from driving the $nsns$-$nsnp$ transition. The time-resolved signal has three components; due to ions, np atoms, and ns atoms, as shown by Fig. 1(b). Driving the $nsns$-$ns(n-1)p$ transition results in an $(n-1)p$ signal which comes after the ns signal. Typically, we sweep the microwave frequency through the atomic ns-np or

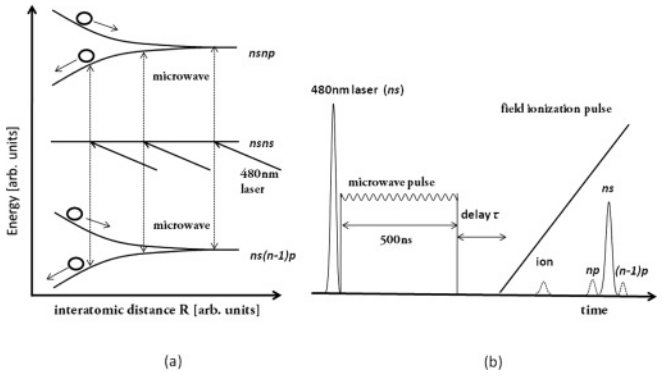

FIG. 1. (a) Typical energy levels for the experiment. The 480-nm laser excites pairs of ns atoms to the $nsns$ potential over a range of internuclear spacings, as shown by the slanted solid line arrows. A microwave pulse, shown by the dotted line arrows, is used to drive the transition to either the $nsnp$ state or the $ns(n-1)p$ state, which can be either attractive or repulsive, depending on the microwave frequency. Pairs excited to a repulsive potential move apart, and those excited to an attractive potential collide, resulting in an ion and a more deeply bound atom. (b) Timing diagram for the $nsns$-$nsnp$ transition. The 8-ns long 480-nm laser pulse excites the atoms to the ns state, and it is immediately followed by a 500-ns long microwave pulse which drives $nsns$ pairs to the $nsnp$ state. After a time delay τ a field ramp is applied, and we detect the time resolved signals due to ions, np atoms, and ns atoms.

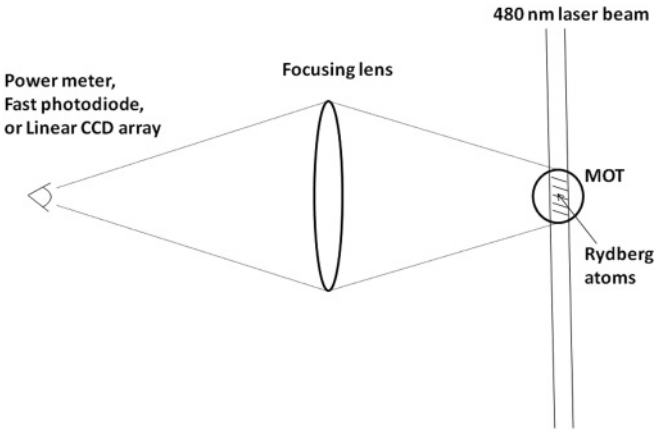

FIG. 2. Measurements of the density of trapped $5p_{3/2}$ and ns Rydberg atoms. A power meter is used to measure the fluorescence power of the MOT. To measure the radius of the MOT, the power meter is replaced by a linear CCD array. The density of the trapped atoms, which is assumed to be a spherical Gaussian cloud, can be determined from these two measurements. Once the number of trapped atoms is known, the number of Rydberg atom can be obtained by measuring the filling time of the MOT and the reduced fluorescence power when the 20 Hz-480 nm excitation laser is sent through the MOT to produce Rydberg atoms. The waist of the 480-nm beam at the focus and the density distribution of atoms in the MOT determines the density distribution of the Rydberg atoms.

ns-$(n-1)p$ resonance over many shots of the laser and detect the ions and np or $(n-1)p$ atoms after a fixed time delay τ.

The general approach for determining the Rydberg atom density in the MOT has been described previously, so the discussion here is brief [13]. A simplified schematic diagram of the measurements is shown in Fig. 2. First, we measure the power of the fluorescence from the trapped atoms into the solid angle subtended by the focusing lens. Assuming that the MOT radiates isotropically, the total fluorescence power is obtained by taking into account the 95% transmission of the lens and the solid angle subtended by the lens at the MOT. Then the total power is divided by the 780-nm power radiated 9.3×10^{-12} W by a single Rb atom to yield the number of trapped atoms. To find the radius of the MOT, we measure its image on a linear charge coupled device (CCD) array. The observed profile is fit to a Gaussian, and its full width at half maximum (FWHM) is extracted, giving the radius $r_M = 380$ μm. These two measurements give us the trap density, which we assume to be spherically symmetric. The number of atoms excited to a Rydberg state is determined from the reduction in number of atoms in the MOT with the 20-Hz excitation laser present and the trap filling time of 0.8 s, which is extracted from the trap filling curve. The volume occupied by the Rydberg atoms is determined by the radius of the MOT and the smaller radius of the 480-nm laser beam $r_L = 70$ μm, which is measured by using the knife-edge scanning method. A knife edge is placed at the focus of the 480-nm beam and the transmission of the laser past the knife edge is recorded as a function of the displacement of the knife edge. The derivative of the transmission is fit to a Gaussian, yielding the diameter of the laser at the center of the MOT. If the laser beam propagates in the z direction, x and y are the perpendicular directions, and

the origin of the coordinate system is at the center of the trap, the density in the trap given by

$$\rho(x,y,z) = \rho_0 e^{-r^2/r_M^2} e^{-(x^2+y^2)/r_L^2}, \quad (1)$$

where the distance from the center of the trap r is defined by $r^2 = x^2 + y^2 + z^2$, and ρ_0 is the density at the center of the trap. In the experiments reported here the peak density ρ_0 of the Rydberg atoms is between 6 and 10×10^9 cm^{-3}. For reference, the average spacing between atoms at a density of 5×10^9 cm^{-3} is 3.6 μm. The excitation to the Rydberg state is done in the presence of the trapping magnetic field to maximize the Rydberg atom density, and the 480-nm light is generated by frequency doubling the pulse amplified output of a single mode continuous wave 960-nm diode laser. The 480-nm pulses have energies of up to 100 μJ, and sweeping the laser frequency across the Rb $5p_{3/2}$–$38s$ transition gives a 110(10)-MHz wide resonance, consistent with the 10-ns duration of the pump pulses for the dye amplifier. The transition is evidently not power broadened, which precludes effects from the ac Stark shifts due to the laser, as discussed by Nascimento *et al.* [12]. The shot-to-shot variation in the number of Rydberg atoms is $\pm 10\%$. Although this variation seems small, its effects are nonetheless quite visible. Due to the inhomogeneous magnetic trapping field the minimum width of the ns-np resonances is 4 MHz, and to make quantitative measurements we generally use the maximum microwave power which does not increase the low density $\rho_0 \sim 10^8$ cm^{-3} resonance linewidth above this value. However, it is useful in some cases to use higher powers.

III. OBSERVATIONS

A graphic demonstration of the difference between the attractive and repulsive potentials is shown in Fig. 3. The data shown in Fig. 3 were taken with high-enough power that the resonances were power broadened to a width of 10 MHz with a low-density atomic sample. For transitions to attractive potentials, higher microwave powers lead to increases in the ion signal since a larger range of internuclear distance can be sampled. Figure 3(a) shows a sweep of the microwave frequency through the atomic $40s$ to $40p$ transition, or the molecular $40s40s$ to $40s40p$ transition while detecting the ions which have been produced after a delay τ of 5 μs. At all microwave frequencies there are ions present, due to the ionization of $40s$ atoms, and this background ion signal has been subtracted. As shown, an increased number of ions is observed when the microwave frequency is below the $40s$–$40p$ frequency of 61 332 MHz so that $40s40s$ pairs are excited to the attractive $40s40p$ potentials. The ion signal falls sharply to the background level at the atomic frequency. Evidently exciting pairs of atoms to the repulsive potential has no observable effect. Although the absorption of the microwave photon increases the energy of one of the atoms, the increased energy has nothing to do with the increase in ion production. To emphasize this point we show the resulting ion signal when the microwave frequency is swept through the $40s \rightarrow 39p$ resonance in Fig. 3(b). The $39p$ state lies below the $40p$ state, and ions are only observed when the microwave frequency is above the atomic $40s$–$39p$ frequency of 70 262 MHz, driving transitions of $40s40s$ pairs to the attractive $40s39p$ potential, as shown in Fig. 1(a). Again, there is no obvious ion production due to the excitation to the repulsive $40s39p$ potential. From Fig. 3 we can obtain a crude estimate of the initial separations of the atoms which are ionized. In Fig. 3(b) the ion signal has its half maximum points at the atomic frequency and 100 MHz above the atomic frequency. The midpoint occurs 50 MHz above the atomic frequency. Using the average attractive dipole-dipole shift we convert the frequency shift of 50 MHz into an interatomic spacing of 3.6 μm. According to the model discussed later, a pair of atoms 3.6 μm apart does collide in 5 μs, so this estimate is reasonable.

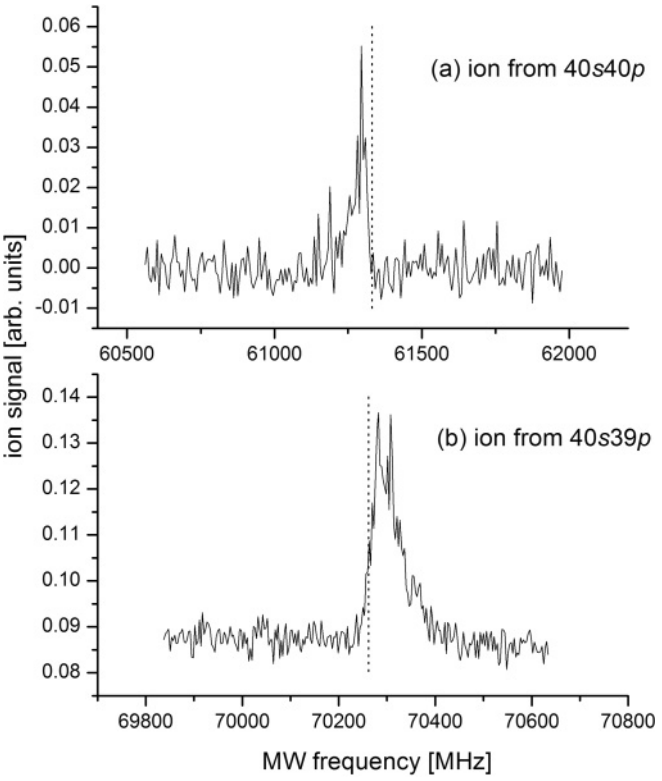

FIG. 3. Ion signals obtained with a delay of 5 μs and a microwave power producing a 10 MHz linewidth after excitation to the $40s$ state. (a) Ion signal obtained in the vicinity of the $40s$–$40p$ transition at 61 332 MHz. (b) Ion signal in the vicinity of the $40s$–$39p$ transition at 70 262 MHz. Although the former transition is to a state of higher energy and the latter to a state of lower energy, in both cases the ions are observed only on the attractive potentials.

To provide a more quantitative picture we have made a systematic study of the evolution of atoms initially excited to the $41s$ state and exposed to a microwave pulse to drive the atoms to the $41p$ state. First, to determine the maximum microwave power that produces a transform limited linewidth of a 500-ns pulse, we turned off the magnetic field 6 ms before the 480-nm laser and reduced the microwave power until we observed a 2-MHz linewidth for the $41s$–$41p$ resonance with a low atomic density. Under the same experimental conditions, a 4-MHz linewidth for the transition was observed when the magnetic field was turned back on. Then, using a high density of atoms and the same microwave power we simultaneously recorded the signals of $41p$ atoms and ions for a series of time delays τ as the microwave frequency was swept through

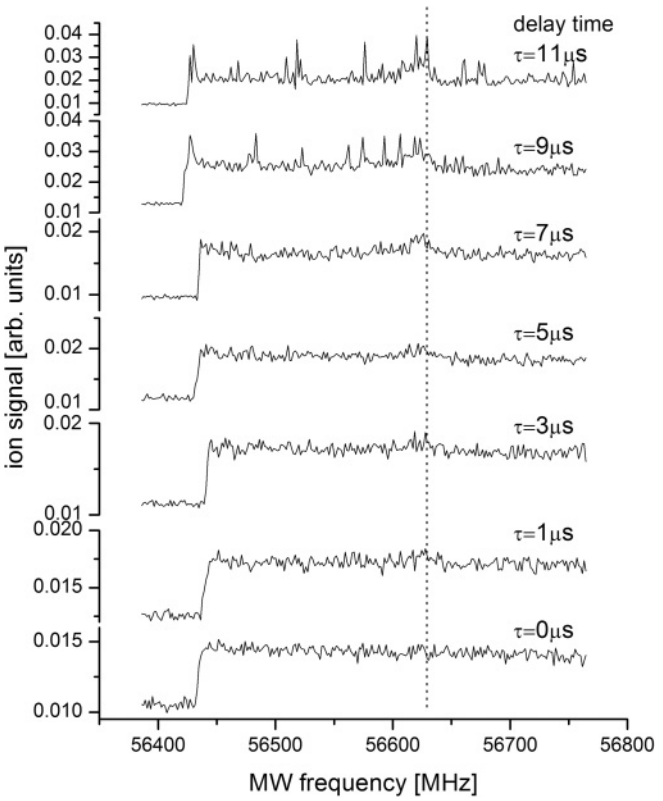

FIG. 4. Ion signals vs microwave frequency observed subsequent to a delay τ after driving the $41s41s$ to $41s41p$ transition. The peak Rydberg atom density is $\rho_0 = 6 \times 10^9$ cm^{-3}. The delay time τ is raised from 0 to 11 μs. Traces for later times are offset vertically and are on coarser scales. The left-hand side of each trace shows the zero signal level. The off-resonant, or background, ion signal rises monotonically with delay time, and for $\tau \geqslant 5$ μs there is a visible increase in the number of ions at frequencies just below the atomic $41s$–$41p$ transition at 56 629 MHz. For delays of 9 and 11 μs the ion signals are obvious. Also obvious in the 9 and 11 μs traces are the random spikes in the ion signal. They originate from the spontaneous evolution to a plasma on intense shots of the laser which lead to an abnormally large number of $41s$ atoms.

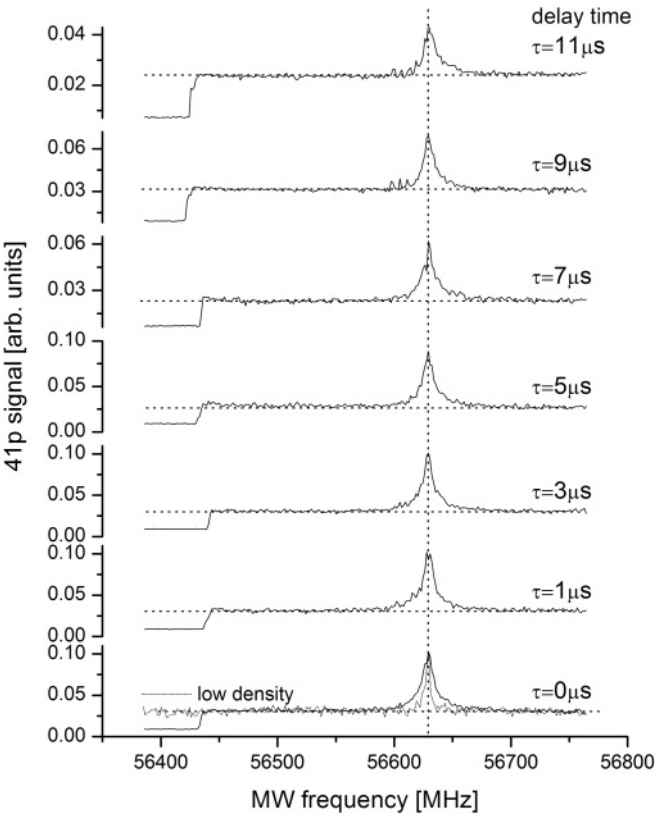

FIG. 5. $41p$ signals vs microwave frequency observed simultaneously with the ion signals of Fig. 3. The time delay τ increases from 0 to 11 μs. Traces for later times are offset vertically. The left-hand side of each trace shows the zero signal level. The off-resonant, or background, $41p$ signal increases until the delay reaches 5 μs, then it decreases. With short delay times the observed lineshape is very nearly symmetric, but when the delay is longer than 5 μs the low-frequency side of the lineshape begins to disappear since pairs excited to the attractive potential are lost to ionization. For reference, for $\tau = 0$ μs we show by a light trace the rescaled low-density signal obtained with the same microwave power.

the atomic $41s$–$41p$ frequency. In terms of Fig. 1, $41s41s$ pairs are driven to the $41s41p$ state and left for time τ before the application of a field ionization pulse. In Fig. 4 we show the ion signals observed for $\tau = 0$ to 11 μs. In each trace of Fig. 4 the zero of the signal is shown on the left-hand side of the trace, and it is evident that the number of ions produced when the microwaves are far off resonance increases with τ. While the source of the ions at $\tau = 0$ is not completely understood, for $\tau = 0$, no additional ions are produced at resonance. For $\tau > 0$ additional ions are observed on the low-frequency side of the atomic resonance frequency, and they are most apparent for $\tau \geqslant 5$ μs. As τ is increased beyond 5 μs progressively more ions are observed on the low-frequency side of the atomic frequency, but no additional ions are observed on the high-frequency side of the atomic resonance. For $\tau = 9$ and 11 μs spikes in the ion signal are observed at random tunings. These spikes are due to the spontaneous evolution to a plasma on laser shots of high intensity. At delays longer than 11 μs the spontaneous evolution to a plasma masks other processes, limiting the range of usable delay times. In Fig. 5 we show the $41p$ signals detected simultaneously with the ion signals of Fig. 4. For $\tau = 0$ we observe a symmetric $41s41s$–$41s41p$ transition lineshape, and as the delay is increased beyond $\tau = 5$ μs, when the $41p$ atoms are detected the lineshape of the resonance becomes progressively more asymmetric due to losing $41s41p$ pairs to ionization on the low-frequency side of the resonance.

IV. MODELING

The experimental data of Figs. 3 and 4 show very clearly that when pairs of atoms are placed on an attractive dipole-dipole potential and allowed time to collide, ionization occurs. The notion that cold atoms move due to attractive dipole-dipole potentials is not new [14,15], and other examples of motion on Rydberg-Rydberg potentials have been observed [16,17]. It is straightforward to compute the time required to collide and ionize, assuming the atoms to be initially at rest, and the result suggests that times far longer than 10 μs are required [6,18]. Most of the time elapses when the atoms are far apart and

moving slowly, an observation which suggests that the initial thermal motion of the atoms is important. When we take it into account in a simple model similar to Robicheaux's we find reasonable agreement between the the experimental data and our model [18].

The model is straightforward. When the spin-orbit interaction of the np state is taken into account we find that of the $ns_{1/2}np_{1/2}$ molecular states there are two with attractive dipole-dipole potentials, which are given by

$$\Phi_{dd} = \frac{\alpha n^4}{R^3}, \tag{2}$$

with $\alpha = -2/9$ and $\alpha = -4/9$. In both cases $|\alpha| < 1$ since the dipole-dipole potentials are not as strong as those of spinless atoms. We use atomic units unless noted otherwise. We begin by computing classically the time required for two atoms on one of these attractive potentials to collide, taking into account the initial thermal velocity of the atoms and assuming that the pair remains on the same potential. The Lagrangian of the two atom system is given by

$$L = T - V = \frac{1}{2}M\dot{R}^2 + \frac{1}{2}Mv_t^2 + \frac{\alpha n^4}{R^3}, \tag{3}$$

where T is the kinetic energy, V the potential energy, R the interatomic distance, M the reduced mass of the two atom pair, half the mass of a Rb atom, and v_t the relative velocity perpendicular to the internuclear axis. The second term on the right-hand side can be written in terms of the angular momentum ℓ, which is given by

$$\ell = MRv_t \tag{4}$$

and is conserved. Using ℓ the equation of the motion can be written as

$$M\ddot{R} - \frac{l^2}{MR^3} + \frac{3\alpha n^4}{R^4} = 0, \tag{5}$$

and the equivalent potential is

$$\phi(R) = \frac{l^2}{2\mu R^2} - \frac{\alpha n^4}{R^3}. \tag{6}$$

Using the fact that ℓ is conserved we write it in terms of the initial value of R, R_i, and the initital value of v_t, v_{ti}. Taking the most probable v_{ti} as $\sqrt{\frac{kT}{M}}$, $\phi(R)$ can be written as

$$\phi(R) = \frac{R_i^2 kT}{2R^2} - \frac{\alpha n^4}{R^3}. \tag{7}$$

The time to collide for the pair of atoms in the potential $\phi(R)$ is given by

$$\tau = \int_{R=0}^{R_i} dt = \sqrt{\frac{2}{M}} \int_{R=0}^{R_i} \frac{dR}{\sqrt{\phi(R_i) - \phi(R) + \frac{1}{2}Mv_{Ri}^2}}, \tag{8}$$

where v_{Ri} is the initial relative velocity along the internuclear axis, which we assume to be in the $-R$ direction. It is convenient to specify $\frac{1}{2}Mv_{Ri}^2 = \beta kT$, where β ranges from 0 to ∞. Finally, the average collision time $\tau_{av}(R_i)$ is given by

$$\tau_{av}(R_i) = \frac{\sqrt{\frac{2}{\mu}} \int_{\beta=0}^{\infty} \int_{R=0}^{R_i} \frac{e^{-\beta/kT} d\beta dR}{\sqrt{\frac{kT}{2} - \frac{\alpha n^4}{R_i^3} - \frac{R_i^2 kT}{2R^2} + \frac{\alpha n^4}{R^3} + \beta kT}}}{\int_0^{\infty} e^{-\beta/kT} d\beta}. \tag{9}$$

In the experiment the maximum collision time is fixed by the delay τ before the application of the field ionization pulse. As a consequence, we invert Eq. (9) to find the maximum spacing between atoms $R_{\max}(\tau)$ which will lead to an ionizing collision in a time τ. This distance in turn defines the minimum frequency shift, or cutoff frequency, $\nu_c(R_{\max})$ for which an ionizing collision will occur with the delay time τ. It is given by

$$\nu_c(R_{\max}) = \frac{\alpha n^4}{R_{\max}^3}. \tag{10}$$

The next step is to calculate the lineshape of the $nsns$ to $nsnp$ transition. Since this procedure has been discussed previously, only a brief summary is provided here [13]. First, energy eigenvalues and eigenfunctions of the $nsns$ and $nsnp$ states are calculated taking into account the dipole-dipole and spin-orbit interactions. The values $\alpha = -2/9$ and $\alpha = -4/9$ are obtained from the eigenvalues. Combining the eigenvalue, or equivalently the frequency shift, with the distribution of atomic spacings implied by the density distribution of the Rydberg atoms, $\rho(r)$, given in Eq. (1), and the peak density ρ_0 yields the infinite resolution lineshape of the transition from $nsns$ to $nsnp$. For the $nsnp$ state with $\alpha = -2/9$ it is shown in Fig. 6(a) by the light solid line. For a delay time $\tau = 9$ μs the cutoff frequency is $\nu_c = 4.5$ MHz, and only transitions to pairs with shifts in excess of this value lead to ionization. Consequently, only the truncated lineshape shown by the bold line in Fig. 6(a) leads to ionization. Finally, the truncated lineshape is convoluted with a 4-MHz linewidth Lorentzian function, shown in Fig. 6(b), since a 4-MHz-Lorentzian line is observed at $\tau = 0$ and low atomic density. The result

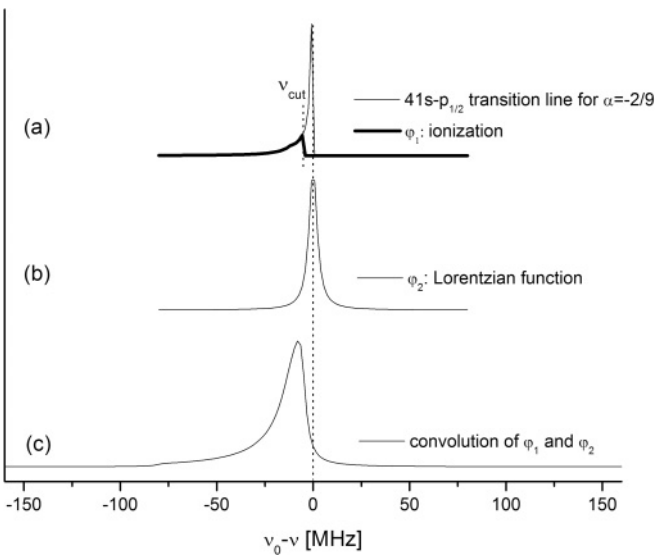

FIG. 6. Construction of the ion signal after a 9 μs delay for the $41s41p$ state with $\alpha = -2/9$. (a) (light line) Infinite resolution spectrum expected for the distribution of atoms in our trap (bold line). The ionization signal comes only from atoms which collide in 9 μs (i.e., only from frequencies $\nu \leqslant \nu_{\rm cut}$). (b) 4 MHz Lorentzian representing the experimental resolution. (c) Convolution of (a) and (b), which is the contribution to the ion signal from the $41s41p$ state with $\alpha = -2/9$. There is an analogous contribution for the state with $\alpha = -4/9$.

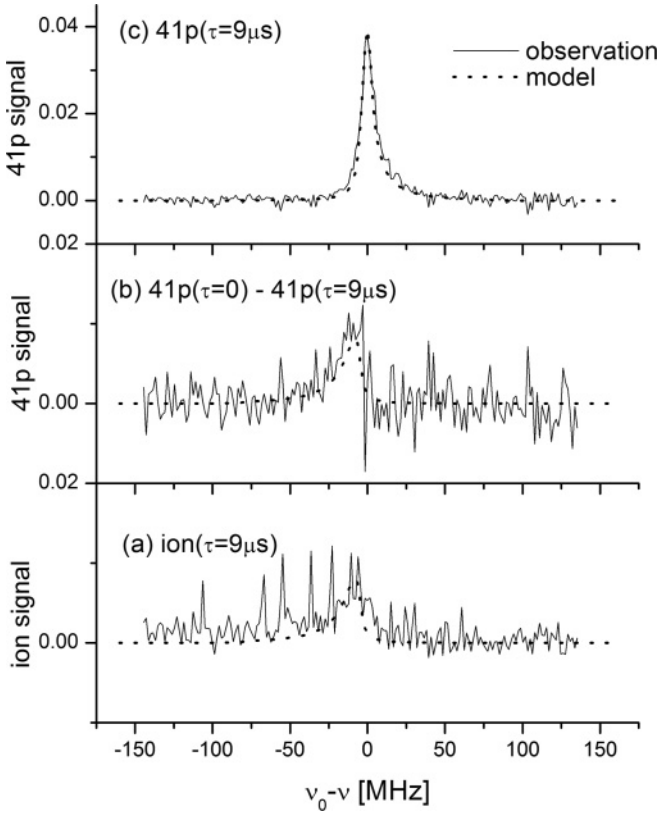

FIG. 7. Observed and calculated signals obtained using the $41s$ state after a delay of 9 μs before the field ionization pulse. (a) Observed (solid line) and calculated (dotted line) ion signals. The random spikes are due to spontaneous evolution to a plasma on unusually intense shots of the laser. (b) Observed difference between the scaled zero delay and 9 μs delay $41p$ signals (solid line) and calculated ion signal (dotted line). (c) Observed (solid line) and calculated (dotted line) $41p$ signals.

is shown in Fig. 6(c), which is the contribution to the ion signal due to the $nsnp$ state with $\alpha = -2/9$ versus microwave frequency. The total ion signal is obtained by computing the ion signal due to the $nsnp$ state with $\alpha = -4/9$ and adding the two signals weighted by their transition strengths. Using perturbation theory with the $nsns$ and $nsnp$ wave functions we can easily calculate the relative transition strengths from the $nsns$ to the $nsnp$ states [13].

In Fig. 7(a), we compare the ion signal observed with a time delay of 9 μs to the one computed using our model. As shown, the agreement is quite good. Moreover, since ionization corresponds to a loss of $41p$ signal, the decrease in the $41p$ signal after a 9-μs time delay is expected to be the same as the ion signal. To verify this, we subtract the $41p$ signal at $\tau = 9\,\mu$s from the scaled $41p$ signal at $\tau = 0$ and compare it to the ionization model, as shown in Fig. 7(b). The agreement is again good. The lineshape of the $41p$ signal at $\tau = 9\,\mu$s can also be generated directly by the model in the following way. For each value of α, both attractive and repulsive, the lineshape analogous to that shown in Fig. 6(a) is computed. For the attractive potentials ($\alpha < 0$) the portions with $\nu < \nu_0$ are removed since those atoms are lost to ionization. In terms of Fig. 6(a) the bold curve is removed. The result is then convoluted with a 4-MHz wide Lorentzian. This procedure is followed for each value of α, and the resulting lineshapes for all values of α are added to obtain the final lineshape. The final lineshape model of the $41p$ signal agrees well with the observation, as shown in Fig. 7(c).

V. HIGH MICROWAVE POWER OBSERVATIONS

To make quantitative measurements of the ionization we kept the microwave power low enough that the linewidth of the microwave resonance with a low-density atomic sample was 4 MHz. This microwave power with the linewidth in turn ensured that we sampled a 4-MHz range of frequency shift, which limited the range of internuclear spacing sampled by any microwave frequency. Raising the microwave power increases the Rabi frequency and increases the range of internuclear spacings sampled at any microwave frequency. As a result, more ions are produced at any microwave frequency, and the Rydberg atom sample is more likely to evolve into a plasma. High-power microwave transitions are thus useful to stimulate the evolution of a Rydberg sample into a plasma, and they can also be used to show definitively that the excitation of pairs to a repulsive dipole-dipole state does not lead to increased ionization on the time scale of these experiments.

To illustrate these phenomena we show in Fig. 8 the effect of driving the $41s$–$41p$ transition with three relatively high microwave field amplitudes and waiting for 7 μs before applying the field ionization pulse. As shown by Fig. 4, there is not much ionization at this delay time with low microwave power. In Fig. 8 we label the three fields E_0, $2E_0$, and $4E_0$, which differ in Rabi frequencies by factors of 2. The microwave field strength E_0 is that used to obtain the data shown in Figs. 4 and 5. The ion signals for these three fields are shown in Figs. 8(a), 8(c), and 8(e). In Fig. 8(a), obtained with E_0, there is a small amount of ionization on the low-frequency side of the atomic frequency, as expected from Fig. 4. In Fig. 8(c), obtained with $2E_0$ there is a noticeable increase in the number of ions detected at frequencies below the atomic frequency due to sampling more values of R at every microwave frequency. In Fig. 8(e), obtained with $4E_0$, the ion signal is very large on the low-frequency side of the atomic resonance, too large to be accounted for simply by motion along the attractive potential followed by ionization. In fact, in this case the Rydberg sample has substantially evolved into a plasma. Equally important, in Fig. 8(e) there is no ionization at frequencies above the atomic frequency, that is, for the excitation of $41s41p$ states on a repulsive potential, in spite of the fact that atoms can be excited to a broad range of internuclear separations. This observation is definitive evidence that excitation to a repulsive potential does not increase the ionization rate. The $41p$ signals were recorded simultaneously with the ion signals, and they are shown in Figs. 8(b), 8(d), and 8(f). In all cases the lineshapes for zero delay $\tau = 0$ are shown as broken lines, and the 7-μs delay signals are shown as solid lines. In Fig. 7(b), obtained with E_0, there is a slight asymmetry due to ionization's removing some of the low-frequency side of the line. In Fig. 8(d), obtained with $2E_0$, the asymmetry is more pronounced, and at frequencies below the resonance frequency the $41p$ signal goes slightly below the off resonance $41p$ baseline signal. In Fig. 8(f), taken

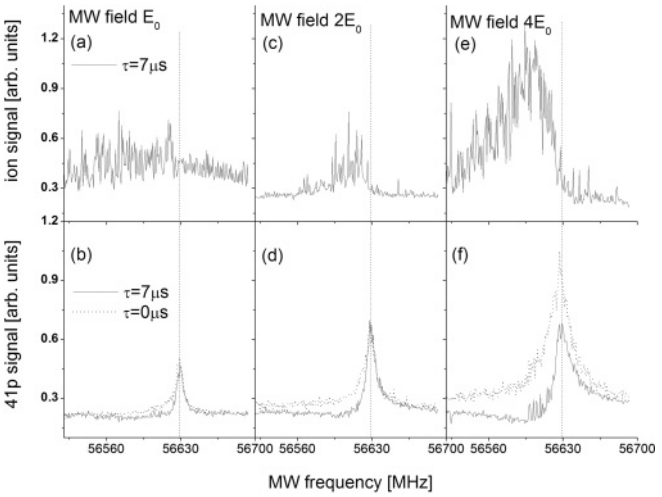

FIG. 8. Observed ion and 41p signals after a delay of 7 μs at three microwave powers leading to linewidths of 4, 8, and 16 MHz with low-density atomic samples showing the evolution to a plasma following the high-power microwave pulse. The peak Rydberg atom density is $\rho_0 = 1 \times 10^{10}$ cm^{-3}. In all cases the atomic 41s–41p transition frequency 56 629 MHz is shown by the broken vertical line. (a) Ion signal with a microwave field amplitude leading to a 4-MHz linewidth. At frequencies below the atomic transition frequency there is more ionization, but only on intense shots of the laser. (b) 41p signals taken with a microwave field amplitude leading to a 4-MHz linewidth with 0 (dotted line) and 7 μs (solid line) delays. With no delay the lineshape is symmetric, but there is a noticeable asymmetry after 7 μs. (c) Ion signal with a microwave field amplitude leading to an 8-MHz linewidth. There is now a clearly visible ion signal over a frequency band 50-MHz wide below the atomic frequency. (d) 41p signals taken with a microwave field amplitude leading to an 8-MHz linewidth with 0 (dotted line) and 7 μs (solid line) delays. With no delay the lineshape is again symmetric, but there is a pronounced asymmetry after 7 μs. In addition, the signal goes slightly below the off-resonant baseline at frequencies just below the atomic frequency. (e) Ion signal with a microwave field amplitude leading to a 16-MHz linewidth. The ion signal now extends over a 100-MHz wide frequency band, and it is too large to be accounted for by only the atoms which have followed attractive potentials and collided. The collisional avalanche creating the plasma is underway. In spite of the fact that a range of internuclear spacing is addressed by this high microwave field, there is no ionization following excitation to the repulsive potential. (g) 41p signals taken with a microwave field amplitude leading to a 16-MHz linewidth with 0 (dotted line) and 7 μs (solid line) delays. With no delay the lineshape is symmetric, but after 7 μs the lineshape has a pronounced asymmetry. In addition it is now clear that below the atomic frequency the 41p signal is far lower than the off-resonant background signal, indicating that a collisional avalanche has started to ionize the background atoms.

with $4E_0$, the dip below the baseline at frequencies below the resonance is obvious, and it is due to the evolution of those atoms into a plasma. The missing atoms in this trace are the source of the large number of ions observed in Fig. 8(e).

As a different probe of the effect of having pairs on different potentials we have observed the ion production after a 7-μs delay with detunings of $\pm$20 MHz, and no microwave field as a function of the number of Rydberg atoms. We have used the same microwave fields used in Fig. 8. As shown in Fig. 9(a),

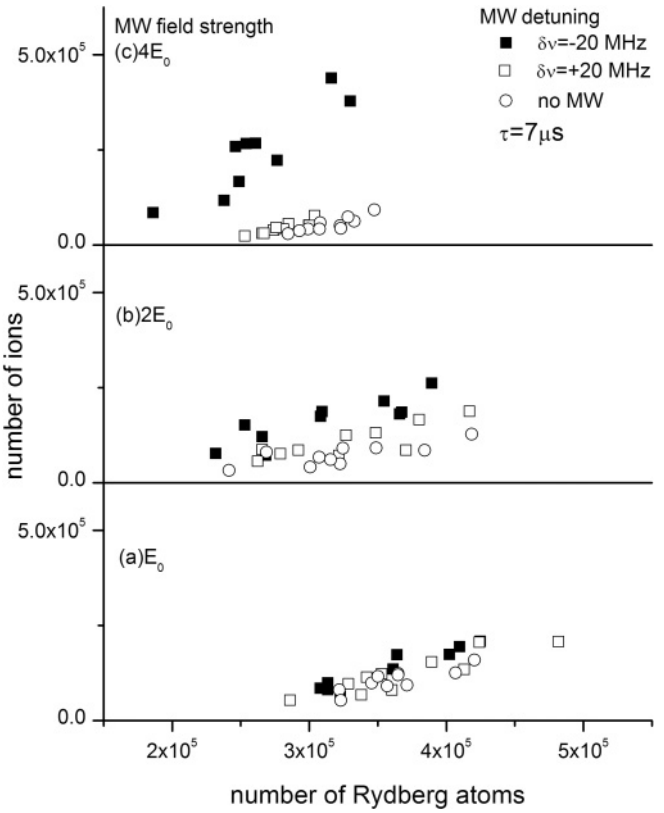

FIG. 9. Ionization signals obtained after 7 μs with no microwaves (◯), +20 MHz, repulsive, detuning (□), −20 MHz, attractive detuning (■), and the three microwave powers producing linewidths of 4, 8, and 16 MHz with low-density atomic samples vs the number of Rydberg atoms initially excited. (a) With a microwave power of 4-MHz linewidth there is a barely discernible difference between tuning to the attractive potential and the other two cases. (b) With a microwave power of 8-MHz linewidth there is now a clear difference between excitation to the attractive potential and the the other two cases, which are indistinguishable. (c) With a microwave power of 16-MHz linewidth there is now a large difference between excitation to the attractive potential and the the other two cases, which are still indistinguishable.

with the microwave field E_0 there is minimal difference between the ion signals observed with no microwaves and the detuned microwave fields, and the number of ions increases roughly linearly with the number of Rydberg atoms. With the microwave field $2E_0$, shown in Fig. 9(b), excitation to the attractive potential with −20 MHz detuning produces more ions than the +20 MHz detuning or no microwaves. In the latter two cases there are no more ions than seen in Fig. 9(a). In Fig. 9(c), obtained with $4E_0$, there is a large ion signal for the −20 MHz detuning, and almost no difference between the signals with a +20 MHz detuning and no microwaves. Again, excitation to the repulsive potential has no effect on the ion production.

VI. DISCUSSION

We have compared the ionization of pairs of atoms on the nearly flat diatomic $nsns$ potential to that observed for pairs on attractive and repulsive $nsnp$ potentials. The latter of these are

reached by a microwave transition from the flat $nsns$ potential. There are several conclusions which can be drawn from this work. First, excitation to an attractive dipole-dipole potential leads to rapid ionization, as expected from previous work [6,8,9]. These measurements show that the initial thermal motion of the atoms significantly shortens the time required for a pair of atoms to collide, and suggests that this form of ionization can be retarded by lower temperatures. For example, if the atoms were initially at 0 K the ion signal shown in Fig. 4 after a delay of 11 μs would require the much longer delay time of 21 μs.

Second, excitation to a repulsive potential does not lead to more ionization than excitation to an essentially flat potential, at least for $n \cong 40$, Rydberg atom densities of $\sim 10^9$ cm^{-3}, and time delays of up to 15 μs. This observation is not so surprising for two reasons. First, the energy gain due to a pair's being on the repulsive potential is small, roughly equivalent to the initial thermal energy. Second, with the 300-μK thermal velocity a time of $\sim$30 μs is required to traverse the average spacing between atoms, so atoms on either $nsns$ or repulsive $nsnp$ potentials are unlikely to collide in the 15-μs duration of our experiments.

The case of most practical interest is that in which the atoms are excited to the same state. Any pair of atoms is either on an attractive or repulsive $1/R^6$ van der Waals potential. If it is attractive the atoms move toward each other, and the van der Waals potential they experience evolves into a $1/R^3$ dipole-dipole potential. Ionization occurs in the time it takes for the atoms to collide. Since the van der Waals potential is flatter at large R than a dipole-dipole potential the initial thermal motion is even more important in reducing the time it takes for the pair of atoms to collide. Other than this difference, the attractive van der Waals and dipole-dipole potentials lead to the same result.

In contrast, ionization by motion on a repulsive van der Waals potential is very different from ionization by motion on a repulsive dipole-dipole potential. Consider two ns atoms A and B in the repulsive $ns_A ns_B$ state. After excitation they separate, and the B atom approaches a third atom C. The $ns_B ns_C$ potential is repulsive, so the B and C atoms can only have an elastic collision. To have an ionizing collision one of the atoms must make a transition to an np state. As pointed out by Amthor *et al.* [10], such a transition can be driven by blackbody radiation [10], a process which occurs at a rate of $\sim 10^3$ s^{-1} at $n = 40$ [4]. In contrast, when atoms A and B on the $ns_A np_B$ repulsive potential separate, atom B can encounter atom C in an ns state, forming a pair on the $np_B ns_C$ potential, which has a 50% chance of being attractive. Whether the $np_B ns_C$ potential is attractive or repulsive depends on the orientations of atoms B and C. If the dipole-dipole $np_B ns_C$ potential is attractive, ionization ensues. The important point is that ionization starting from a repulsive van der Waals potential requires a radiative transition, which appears to be the rate limiting step. In light of this difference, the similarity of our results for $nsns$ and repulsive $nsnp$ potentials is a little surprising, even though the atoms are only allowed a short time to move. We expect that with longer times the difference between the two repulsive potentials will become apparent. However, in our experiments other ionization processes mask the effect of motion on repulsive potentials. For example, the source of the background ions in Figs. 3 and 4 is not yet completely understood.

Finally, it is possible to greatly accelerate the plasma formation with high power microwave excitation since atoms over a wide range of internuclear separations can be simultaneously transferred to attractive potentials.

ACKNOWLEDGMENTS

This work was supported by the Air Force Office of Scientific Research. It is a pleasure to acknowledge helpful discussions with R. R. Jones.

[1] M. P. Robinson, B. Laburthe Tolra, M. W. Noel, T. F. Gallagher, and P. Pillet, Phys. Rev. Lett. **85**, 4466 (2000).
[2] S. K. Dutta, D. Feldbaum, A. Walz-Flannigan, J. R. Guest, and G. Raithel, Phys. Rev. Lett. **86**, 3993 (2001).
[3] W. Li *et al.*, Phys. Rev. A **70**, 042713 (2004).
[4] W. E. Cooke and T. F. Gallagher, Phys. Rev. A **21**, 588 (1980).
[5] B. Knuffman and G. Raithel, Phys. Rev. A **73**, 020704(R) (2006).
[6] W. Li, P. J. Tanner, and T. F. Gallagher, Phys. Rev. Lett. **94**, 173001 (2005).
[7] J. S. Cabral, J. M. Kondo, L. F. Goncalves, L. G. Marcassa, D. Booth, J. Tallant, and J. P. Shaffer, New J. Phys. **12**, 093023 (2010).
[8] T. Amthor, M. Reetz-Lamour, S. Westermann, J. Denskat, and M. Weidemuller, Phys. Rev. Lett. **98**, 023004 (2007).
[9] M. Viteau, A. Chotia, D. Comparat, D. A. Tate, T. F. Gallagher, and P. Pillet, Phys. Rev. A **78**, 040704(R) (2008).
[10] T. Amthor, M. Reetz-Lamour, C. Giese, and M. Weidemuller, Phys. Rev. A **76**, 054702 (2007).
[11] A. Reinhard, K. C. Younge, T. C. Liebisch, B. Knuffman, P. R. Berman, and G. Raithel, Phys. Rev. Lett. **100**, 233201 (2008).
[12] V. A. Nascimento, L. L. Caliri, A. Schwettmann, J. P. Shaffer, and L. G. Marcassa, Phys. Rev. Lett. **102**, 213201 (2009).
[13] H. Park, P. J. Tanner, B. J. Claessens, E. S. Shuman, and T. F. Gallagher, Phys. Rev. A **84**, 022704 (2011).
[14] A. Gallagher and D. E. Pritchard, Phys. Rev. Lett. **63**, 957 (1989).
[15] S. D. Gensemer and P. L. Gould, Phys. Rev. Lett. **80**, 936 (1998).
[16] A. Fioretti, D. Comparat, C. Drag, T. F. Gallagher, and P. Pillet, Phys. Rev. Lett. **82**, 1839 (1999).
[17] K. R. Overstreet, A. Schwettmann, J. Tallant, and J. P. Shaffer, Phys. Rev. A **76**, 011403(R) (2007).
[18] F. Robicheaux, J. Phys. B **38**, S333 (2005).